U.S. ARMY COMBAT CAPABILITIES DEVELOPMENT COMMAND
CHEMICAL BIOLOGICAL CENTER

ABERDEEN PROVING GROUND, MD 21010-5424

DEVCOM CBC-TR-1729

Isoflurane as an Accurate Negative Mode Calibrant for Ion Mobility Spectrometry

Brian C. Hauck
Charles S. Harden

SCIENCE AND TECHNOLOGY CORPORATION
Belcamp, MD 21017-1427

Vincent M. McHugh

RESEARCH AND TECHNOLOGY DIRECTORATE

August 2021

Disclaimer

The findings in this report are not to be construed as an official Department of the Army position unless so designated by other authorizing documents.

REPORT DOCUMENTATION PAGE

Form Approved
OMB No. 0704-0188

1. REPORT DATE *(DD-MM-YYYY)*	**2. REPORT TYPE**	**3. DATES COVERED** *(From - To)*
XX-08-2021	Final	Feb 2019 – Feb 2020

4. TITLE AND SUBTITLE
Isoflurane as an Accurate Negative Mode Calibrant for Ion Mobility Spectrometry

5a. CONTRACT NUMBER

5b. GRANT NUMBER

5c. PROGRAM ELEMENT NUMBER

6. AUTHOR(S)
Hauck, Brian C.; Harden, Charles S. (STC); and McHugh, Vincent M. (DEVCOM CBC)

5d. PROJECT NUMBER

5e. TASK NUMBER

5f. WORK UNIT NUMBER

7. PERFORMING ORGANIZATION NAME(S) AND ADDRESS(ES)
Science and Technology Corporation; 111 C Bata Boulevard, Belcamp, MD 21017-1427
Director, DEVCOM CBC; ATTN: FCDD-CBR-ID, APG, MD 21010-5424

8. PERFORMING ORGANIZATION REPORT NUMBER
DEVCOM CBC-TR-1729

9. SPONSORING / MONITORING AGENCY NAME(S) AND ADDRESS(ES)
Joint Project Manager for Chemical, Biological, Radiological and Nuclear Sensors; APG, MD 21010-5424

10. SPONSOR/MONITOR'S ACRONYM(S)
JPM CBRN Sensors

11. SPONSOR/MONITOR'S REPORT NUMBER(S)

12. DISTRIBUTION / AVAILABILITY STATEMENT
Approved for public release: distribution unlimited.

13. SUPPLEMENTARY NOTES
U.S. Army Combat Capabilities Development Command Chemical Biological Center (DEVCOM CBC) was previously known as U.S. Army Edgewood Chemical Biological Center (ECBC).

14. ABSTRACT: (Limit 200 words)
The search for suitable ion mobility spectrometry (IMS) calibrant compounds is ongoing and neccesitates the use of highly accurate reduced ion mobility (K_0) values across a range of instrumental conditions. Such values will be used in calibrating devices to shift the ion mobility scales and alarm windows for chemicals of interest to their proper locations, based on the instrumental conditions present during calibration and sampling. Many positive ion mode calibrants have been investigated, whereas investigations for a negative ion detection mode calibrant have been more limited. Isoflurane (IsoF) is a strong candidate as a negative ion mode calibrant. This report documents the accurately measured K_0 values for IsoF product ions as a function of multiple instrumental parameters. K_0 values were measured in two instrumentation modes as a function of drift gas temperature, water concentration, and dopant concentration. This report culminates with our evaluation of the suitability of IsoF as a negative ion mode calibrant for IMS applications.

15. SUBJECT TERMS
Ion mobility spectrometry (IMS) | Reference standards | Accuracy | Calibrant
Calibration | Reduced ion mobility (K_0) | Precision

16. SECURITY CLASSIFICATION OF:			**17. LIMITATION OF ABSTRACT**	**18. NUMBER OF PAGES**	**19a. NAME OF RESPONSIBLE PERSON**
a. REPORT	**b. ABSTRACT**	**c. THIS PAGE**			Renu B. Rastogi
U	U	U	UU	34	**19b. TELEPHONE NUMBER** *(include area code)* (410) 436-7545

Blank

PREFACE

The work described in this report was authorized under FY19 Budget Activity 5 Research, Development, Test and Evaluation funds that were issued as an Economy Act Order in accordance with Defense Finance Accounting Service - Indianapolis (DFAS-IN) Manual 37-100 and DoD Financial Management Regulation (FMR) Volume 11. The work was started in February 2019 and completed in February 2020. At the time this work was performed, the U.S. Army Combat Capabilities Development Command Chemical Biological Center (DEVCOM CBC) was known as the U.S. Army Edgewood Chemical Biological Center (ECBC).

The use of either trade or manufacturers' names in this report does not constitute an official endorsement of any commercial products. This report may not be cited for purposes of advertisement.

This report has been approved for public release.

Acknowledgment

The authors acknowledge Jasmine Wilding (Joint Project Manager for Chemical, Biological, Radiological and Nuclear Sensors; Aberdeen Proving Ground, MD) for her assistance in acquiring funding.

Blank

CONTENTS

FIGURES

ISOFLURANE AS AN ACCURATE NEGATIVE MODE CALIBRANT FOR ION MOBILITY SPECTROMETRY

1. INTRODUCTION

Ion mobility spectrometry (IMS) is used in national security applications to detect the presence of illicit substances such as chemical warfare agents, explosives, and toxic industrial chemicals that are harmful to warfighters and end users.[1–3] Using IMS-based detectors such as the Lightweight Chemical Detector (LCD 3.3; Smiths Detection; London, UK) requires that one trust the detection and alarm algorithm to correctly identify threats and sound true-positive alarms and simultaneously minimize false-positive alarms. These false-positive alarms result from erroneous interferents appearing within the relatively wide alarm windows for compounds of interest on the reduced ion mobility (K_0) scale. The K_0 value by which chemicals of interest are identified is calculated from the drift time (t_d) of their ions traveling under an applied voltage gradient (V) across a known length (L), with the pressure (P) and temperature (T) of a countercurrent drift gas normalized against standard pressure and temperature, as shown:[2]

$$K_0 = \frac{L^2}{Vt_d}\left(\frac{273.15}{T}\right)\left(\frac{P}{760}\right) \quad (1)$$

Two components contribute to the current strategy for calibrating IMS-based detectors and minimizing false-positive alarms. First, alarm windows for chemicals of interest are based on K_0 value measurements from multiple detectors and environmental conditions. Second, detectors are exposed to calibrants for both the positive and the negative ion detection modes. "Correction factors" are applied to positive and negative mode ion mobility scales based on the response of each detector to the calibrants. The reference K_0 values used to establish the alarm windows and the correction factors for calibration have historically been accurate, at best, to approximately ±2% of the average. This inaccuracy is what forces the algorithm to use relatively wide alarm windows, again approximately ±2%, to maximize true-positive alarms while minimizing false-negative responses. As a result, the alarm windows for chemicals of interest and known interferents overlap and cause false-positive alarms.[4] However, the overlap between the alarm windows for chemicals of interest and known interferents could be eliminated by reducing their widths by an order of magnitude. The only way to do this is to update the correction factors on an on-demand basis and use high-accuracy reference K_0 values in calibration.

Calibration using high-accuracy reference K_0 values can be achieved with eq 2. In such a calibration scenario, the end user would expose the detector to one or more calibrant compounds that have been accurately characterized across the range of operational parameters for the detector. The algorithm would select the proper high-accuracy calibrant K_0 value for the operational parameters present during calibration (K_{0std}) from an internal library of these accurate K_0 values. The ratio of K_{0std} to the uncalibrated response of the detector to the calibrant (K_{0cal}) is the calibration factor by which all other initially observed K_0 values (K_{0obs}) would be multiplied on the uncalibrated ion mobility scale. Doing so will return a calibrated K_0 value and scale for

detection and identification purposes (K_{0det}). Once the ion mobility scale is calibrated, the algorithm can shift the narrower detection windows to their proper locations based on an internal library of known high-accuracy K_0 values for the chemicals of interest at the same operational conditions. In this way, false-positive alarms are minimized by the narrower alarm windows, and a low rate of false-negative responses is maintained by the shifting of those windows.[4]

$$K_{0\mathrm{det}} = \left(\frac{K_{0\mathrm{std}}}{K_{0\mathrm{cal}}}\right) K_{0\mathrm{obs}} \tag{2}$$

Successful execution of this strategy is reliant on having high-accuracy reference K_0 values for both the calibrants and the chemicals of interest. Recently, multiple potential calibrants were accurately analyzed, and it was concluded that di(propylene glycol) methyl ether (DPM) and 2,6-di-*tert*-butylpyridine (D*t*BP) were the best candidates for the positive ion mode. In the negative ion mode, the identity of methyl salicylate (MES) product ions and their ability to form were found to change as a function of drift gas water concentration.[5] Isoflurane (IsoF), shown in Figure 1, is active in the negative ion mode and was first analyzed by IMS as an occupational hazard for medical personnel because of its primary use as an anesthetic.[6] However, IsoF has since been proposed as a calibrant because it has high electronegativity, high vapor pressure, and relatively low toxicity and it forms monomer and dimer species that can be used for quantification of drift gas water concentration. A potential disadvantage to the use of IsoF as a negative ion mode calibrant is the existence of structural isomers, but this is mitigated by its commercial availability in high purity.[4,7] In this report, we document the accurate and precise K_0 values for IsoF monomer and dimer product ions as a function of drift gas temperature and drift gas water concentration (i.e., relative humidity) using a high-accuracy ion mobility spectrometry time-of-flight mass spectrometry (IMS–TOFMS) instrument. This report also documents our evaluation of the suitability of IsoF as a negative ion mode calibrant for IMS applications.

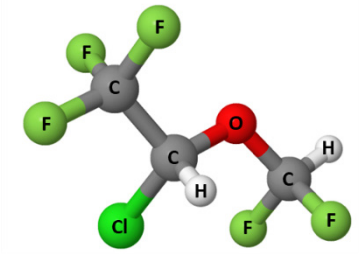

CAS:	26675-46-7
Molecular Formula:	$C_3H_2ClF_5O$
Molecular Weight:	184.49 °C
Boiling Point:	48.5 °C
Density:	1.496 g/mL (25 °C)
Vapor Pressure:	295 mmHg (25°C)

Figure 1. Molecular structure and physical properties of IsoF. Molecular properties are from the safety data sheet. CAS, Chemical Abstracts Service.

2. EXPERIMENTAL SECTION

2.1 IMS–TOFMS Instrument

K_0 values were measured using the previously described Accurate Ion Mobility Instrument (AIMI), which measures and controls the variables shown in eq 1 to an optimized accuracy of ±0.1%.[8] A schematic of the system and its components is shown in the appendix (Figure A-1). The negative mode ionization source was ^{63}Ni because of the formation of NO_x species when corona ionization is used. The length of the drift tube between two Bradbury–Nielson (BN) ion gates was 16.249 ± 0.007 cm at room temperature and was corrected for thermal expansion and contraction. Ion drift times were calculated as the difference between drift time measurements taken from each BN ion gate operated with a 200 μs pulse width. The TOFMS (Ionwerks, Inc.; Houston, TX) mass-identified all ion drift time peaks in an ion mobility–mass spectrometry (IMMS) mode. The AIMI drift tube also contained an annular Faraday plate before the vacuum interface of the TOFMS instrument for standalone analyses. In this standalone IMS mode, the second BN ion gate acted as an aperture grid, and the drift length between the first BN ion gate and the Faraday plate was 16.433 cm, based on 1.477 $cm^2V^{-1}s^{-1}$ as the accurate K_0 value for D*t*BP.[5] Signal from the Faraday plate was amplified by a model 427 current amplifier (Keithley Instruments, Inc.; Cleveland, OH), and spectra were recorded and analyzed using previously written LabVIEW programs (National Instruments; Austin, TX).[9]

The electric field strength of the drift tube was set to 280 V/cm in both instrumentation modes. A custom preheater powered by a Variac transformer and an AD07R-40 refrigerated circulator filled with Polycool HC-50 fluid (PolyScience; Niles, IL) were used to preheat and precool, respectively, the drift gas in conjunction with the drift tube thermal case. Data were collected at 15, 25, 30, 40, and 50 °C, and drift gas temperature gradients were minimized across *L* to within ±0.3 ºC or better. Precise temperature measurements are listed in the appendix (Tables A-1 through A-8). Ambient pressure was measured using a Princo model 453 standard mercurial barometer (Precision Thermometer and Instrument Company; Philadelphia, PA) and was corrected for temperature and latitude at the measurement point.

2.2 Chemicals and Solvents

IsoF was obtained as a European Pharmacopoeia reference standard from Sigma-Aldrich Chemical Company (St. Louis, MO) containing a racemic mixture of (*R*) and (*S*) stereoisomers. Water reactant ions $H^+(H_2O)_n$ were confirmed in the mass mobility spectra under undoped conditions. Under the doped conditions used here, ammonia was introduced into the drift gas using Trace Source disposable ammonia permeation tubes (Kin-Tek; La Marque, TX) that were certified to create a 20 ppmv (parts per million by volume) drift gas dopant concentration at a 1.00 ± 0.01 L/min flow of compressed house air (approximately 1 ppmv H_2O). The flow of drift gas was controlled by an 1179A Mass-Flo digital mass flow controller with a model 247D power supply/readout (MKS Instruments; Andover, MA). When ammonia dopant was generated, reactant ion chemistry favored ammonium reactant ions $H^+(NH_3)_m(H_2O)_n$; *n* was observed to equal 0 in the mass spectrum, but water may have been attached to the ammonium ion in the drift tube before it detached in the mass spectrometer vacuum interface. High-performance liquid chromatography (HPLC)-grade water (Fisher Scientific; Waltham, MA) was introduced as a drift gas modifier to simulate humidity effects on K_0 values.

2.3 Water and Dopant Introduction

Drift gas water concentration was varied between approximately 5 and 550 ppmv by operating a 74900 series single-syringe infusion pump (Cole-Parmer; Vernon Hills, IL) and a 250 µL Gastight no. 1725 syringe (Hamilton Company; Reno, NV) as needed for up to 60 µL/h. A silica capillary (150 µm i.d., 360 µm o.d.; Polymicro Technologies; Phoenix, AZ) was attached to the syringe. The capillary was inserted orthogonally into the drift gas line using Valco Instruments Company, Inc. (Houston, TX) fittings, and HPLC-grade water was pumped into the drift gas before the mass flow controller. During the acquisition of each spectrum, a LabVIEW program recorded the drift gas water concentration measured by a Moisture Image Series 1 hygrometer and probe (GE Measurement and Control; Fairfield, CT). Under ammonia-doped conditions, a permeation tube was inserted into a chamber after the hygrometer probe, and dopant was present in both the drift and reaction regions of the instrument to simulate field detector conditions. The drift gas was not humidified during experiments at 15 °C to prevent electrical arcing within the drift tube.

2.4 Sample Introduction

The septum of a 1.4 mL sample vial was punctured with a needle, and the sample vial was placed in a wash bottle (VWR International; Radnor, PA). The wash bottle was used as needed to flush sample vapor through an EZRU21 external/internal reducing union (Valco Instruments Co.) and silica capillary (150 µm i.d., 360 µm o.d.; Polymicro Technologies). The silica capillary was inserted into the reaction region of the AIMI drift tube via a port in one of the reaction region electrodes.[4] The small-diameter capillary minimized temperature gradients resulting from the introduction of room-temperature sample air.

3. RESULTS AND DISCUSSION

3.1 Ion Chemistry

Reactant ions present in the AIMI drift tube under both dopant conditions were O_2^- (mass-to-charge ratio [*m*/*z*] 32), CO_3^- (*m*/*z* 60), and $N_2O_3^-$ (*m*/*z* 76). Upon introduction of IsoF under dry conditions, multiple product ions were observed with paired masses due to the ^{35}Cl and ^{37}Cl isotopes of IsoF. The main IsoF product ions were an oxygen adduct ($[IsoF{\bullet}O_2]^-$; *m/z* 216, 218), a carbonate adduct ($[IsoF{\bullet}CO_3]^-$; *m/z* 244, 266), and an oxygen bound dimer ($[(IsoF)_2{\bullet}O_2]^-$; *m/z* 400, 402, 404). A nitrate adduct ($[IsoF{\bullet}NO_2]^-$; *m/z* 230, 232) was also present in the mass spectrum, but K_0 values could not be measured in a reasonable amount of time in IMMS mode, and a resolved peak was not produced in standalone IMS mode. Two previous ion mobility studies of IsoF reported similar product ions. Eiceman and colleagues reported the presence of $[IsoF{\bullet}Cl]^-$, $[IsoF{\bullet}N_2O_2]^-$, $[(IsoF)_2{\bullet}O_2]^-$, and $[(IsoF)_2{\bullet}Cl]^-$ in an IMMS instrument operated at an electric field strength of 215 V/cm at ambient pressure and 40 °C, using a ^{63}Ni ionization source and compressed air as the drift gas. However, the authors noted that all product ions and associated reactant ions except for $[(IsoF)_2{\bullet}O_2]^-$ were a result of latent chloride contamination from previous experiments.[6] González-Méndez and colleagues reported the presence of $[IsoF{\bullet}O_2]^-$ and $[(IsoF)_2{\bullet}O_2]^-$ on their IMS-quadrupole MS instrument operated at an

electric field strength of 200 V/cm at ambient pressure and 30 ± 1 °C, with a ^{63}Ni ionization source and both zero-air and pure nitrogen drift gases.[7] The authors did not report the presence of $[IsoF{\bullet}CO_3]^-$, but this may be because it did not form a resolved ion mobility peak. An additional study by González-Méndez and colleagues reports K_0 values for IsoF; however, the mass-identified ion mobility peaks were chloride species resulting from the use of a hexachloroethane dopant.[10]

When IsoF was introduced into the AIMI drift tube, $[(IsoF)_2{\bullet}O_2]^-$ formed; at high IsoF concentrations, it eliminated the reactant ion and $[IsoF{\bullet}O_2]^-$ peaks. However, the $[IsoF{\bullet}CO_3]^-$ peak height did not decrease as the $[(IsoF)_2{\bullet}O_2]^-$ peak height increased. This is shown in Figure 2 with three standalone IMS mode spectra corresponding to low (blue), medium (purple), and high (red) IsoF vapor concentrations. These IsoF vapor concentrations were not quantified; rather, they were indicated by the length or number of times the sample wash bottle was squeezed during the course of the recorded spectra. The $[IsoF{\bullet}O_2]^-$ and $[IsoF{\bullet}CO_3]^-$ peaks were not fully resolved. These peaks would also be unresolved in common handheld IMS-based detectors, given their shorter drift tube lengths and lower resolving power. As a result, upon first administration of IsoF as a calibrant and production of a high dimer product ion peak, IsoF would appear to shift the monomer peak to a longer drift time and lower K_0 value as a function of increasing concentration. It will therefore be imperative to account for this phenomenon in the calibration algorithm by having the program only select calibration spectra that fall within a predetermined acceptable range of monomer-to-dimer peak height ratios.

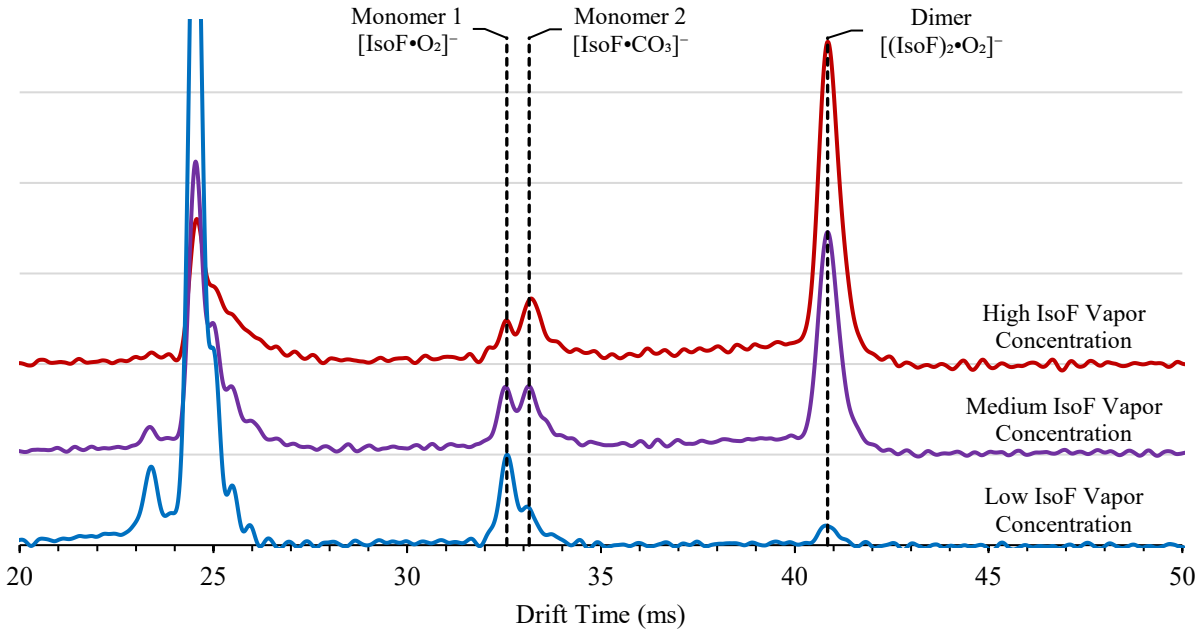

Figure 2. Standalone IMS spectra of IsoF (30.07 ± 0.03 °C, 0.99 ± 0.08 ppmv H_2O, 280.1 V/cm, 20 ppmv ammonia dopant) when introduced at low (blue), medium (purple), and high (red) analyte concentrations in IMMS mode.

Although stable product ions are shown in Figure 2 under dry drift gas conditions, an increase in drift gas water concentration affected the stability of IsoF product ion complexes. Figure 3 shows seven consecutive standalone IMS spectra at increasing drift gas water concentrations and all at 25 °C. Under the driest conditions (0.799 ± 0.001 ppmv H_2O), strong monomer and dimer peaks were formed corresponding to $[IsoF•O_2]^-$ and $[(IsoF)_2•O_2]^-$, respectively. A small shoulder corresponding to $[IsoF•CO_3]^-$ formed on the tailing edge of the $[IsoF•O_2]^-$ peak. However, as drift gas water concentration increased, water molecules clustering around $[IsoF•O_2]^-$ prevented the attachment of a second IsoF molecule to the monomer ion. As a result, more IsoF vapor (multiple squeezes of the sample wash bottle) was required to form $[(IsoF)_2•O_2]^-$ at higher water vapor concentrations. The bridging observed between the monomer and dimer drift time peaks was a result of unstable complexes that formed and fragmented while traveling down the drift region and consisted of multiple neutral water molecules and $[IsoF•O_2]^-$. It is also possible that additional IsoF molecules attempting to form $[(IsoF)_2•O_2]^-$ contributed to these unstable complexes. The degree of bridging increased as drift gas water concentration increased, until ultimately, a stable $[(IsoF)_2•O_2]^-$ ion and peak could not be formed. Attempts to form $[(IsoF)_2•O_2]^-$ at these highest drift gas water concentrations instead eliminated the reactant ion and $[IsoF•O_2]^-$ peaks in favor of unstable complexes along the drift time axis. However, the drift gas water concentrations at which this effect occurred would be reached after the drift gas molecular sieve pack in a handheld detector would be expended. This indicates that IsoF would be a stable and acceptable calibrant under a limited range of drift gas water concentrations.

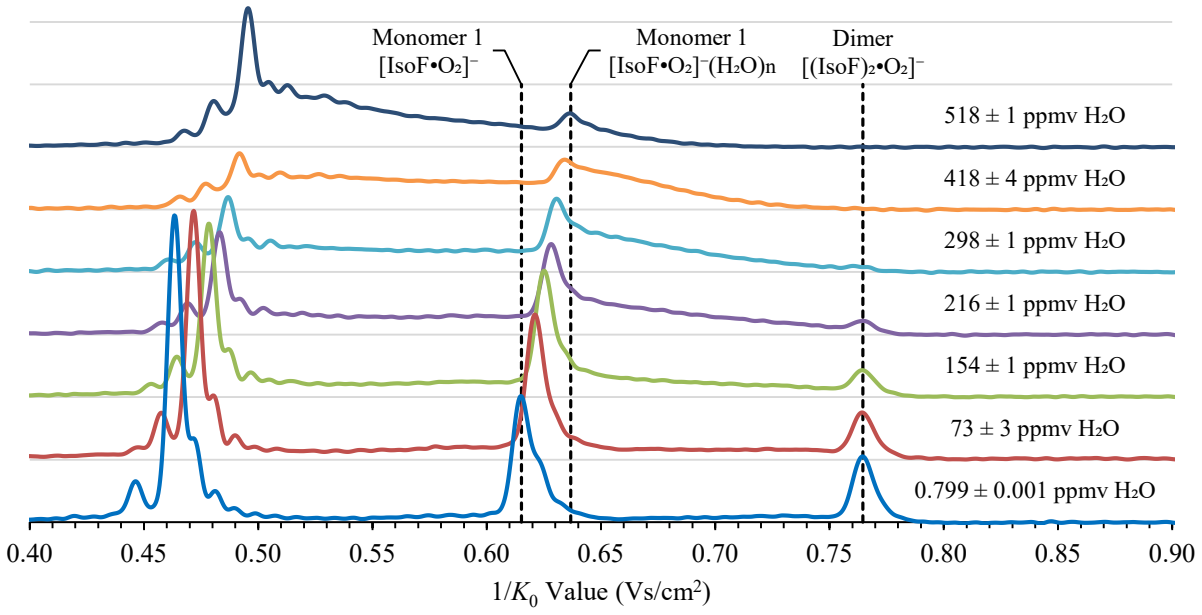

Figure 3. Standalone IMS spectra of IsoF (25.00 ± 0.08 °C, 280.2 V/cm, 20 ppmv ammonia dopant) at seven drift gas water concentrations.

3.2 K_0 Values for Product Ions

3.2.1 $[IsoF•O_2]^-$ Monomer

Figure 4 shows the effect of drift gas temperature and water concentration on the K_0 value for $[IsoF•O_2]^-$ in the IMMS mode under both ammonia-doped (solid marker) and undoped (open marker) conditions. $[IsoF•O_2]^-$ formed under all drift gas conditions and its K_0 value decreased, in a quadratic fashion, between 3 and 4% as a function of increasing drift gas water concentration at each drift gas temperature. Ammonia dopant did not have an effect on the K_0 value for $[IsoF•O_2]^-$, as each trend line in Figure 4 incorporates the ammonia-doped and undoped K_0 values; data points at relatively the same drift gas water concentration conditions agreed under ammonia-doped and undoped conditions. Data collected with the Faraday plate in standalone IMS mode under the same drift gas conditions are shown in appendix Figure A-2. The values in Figure A-2 are consistent with those shown in Figure 4 and indicate that the TOFMS instrument did not affect ion K_0 values.

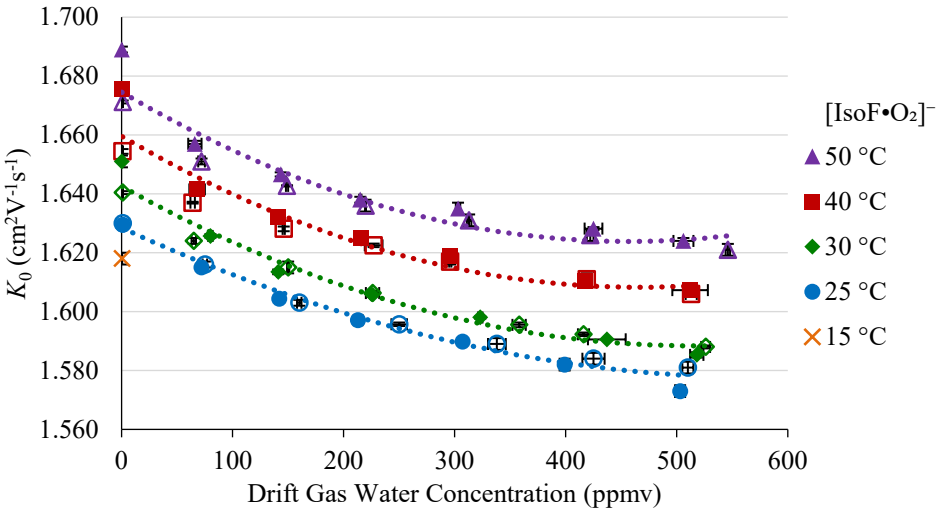

Figure 4. Effect of drift gas water concentration on the K_0 value for $[IsoF•O_2]^-$ in IMMS mode at five drift gas temperatures under ammonia-doped (solid marker) and undoped (open marker) conditions.

Of the two IsoF studies previously mentioned, only González-Méndez and colleagues[7] reported the presence of $[IsoF•O_2]^-$ with a K_0 value of 1.51 $cm^2V^{-1}s^{-1}$. The comparable undoped IMMS mode K_0 value for $[IsoF•O_2]^-$ at 30.02 ± 0.03 °C and 1.00 ± 0.02 ppmv H_2O was 1.6404 ± 0.0005 $cm^2V^{-1}s^{-1}$. This was an 8.6% increase in the value as reported by González-Méndez and colleagues. This increase may have resulted from a combination of inaccuracies in their instrumental measurements, such as the drift length or temperature gradient, which could have lowered their calculated K_0 value in error. Another source of inaccuracy may have been the unrecognized presence of $[IsoF•CO_3]^-$ monomer in their ion mobility spectrum. Although $[IsoF•CO_3]^-$ was not predicted in their density functional theory calculations, the two spectra in Figure 2 of their report showed a high dimer peak amplitude and

a broader monomer peak with a lower amplitude. Their reactant ion, monomer, and dimer peak height ratios most resembled the medium and high IsoF vapor concentration spectra reported here (Figure 2). As previously discussed, a relatively high concentration of IsoF in their drift tube may have shifted the monomer peak from $[IsoF•O_2]^-$ to $[IsoF•CO_3]^-$, which is a larger ion with a lower K_0 value, or formed an unresolved peak that had a K_0 value between the two.

3.2.2 $[IsoF•CO_3]^-$ Monomer

In Figure 5, the K_0 value for $[IsoF•CO_3]^-$ is reported as a function of drift gas temperature and water concentration in IMMS mode under both ammonia-doped (solid marker) and undoped (open marker) conditions. No other known study has reported observations of $[IsoF•CO_3]^-$; therefore, there are no previously reported K_0 values with which to compare these measurements. The highest and lowest observed K_0 values for $[IsoF•CO_3]^-$ in IMMS mode under ammonia-doped conditions were 1.627 ± 0.001 and 1.5998 ± 0.0005 $cm^2V^{-1}s^{-1}$ at 50.01 ± 0.04 °C (0.25 ± 0.01 ppmv H_2O) and 25.0 ± 0.08 °C (142 ± 3 ppmv H_2O), respectively. Similar to the results for $[IsoF•O_2]^-$, there was no significant difference in K_0 values between ammonia-doped and undoped conditions for $[IsoF•CO_3]^-$. The 25 °C trend line in Figure 5 appears to be quadratic, whereas the remaining trend lines are linear. K_0 values for the corresponding second monomer peak (i.e., $[IsoF•CO_3]^-$) were measured in standalone IMS mode, and are included in appendix Tables A-7 and A-8. However, these standalone IMS mode K_0 values were not plotted in Figure 5 because they were consistent with the values already plotted and could only be measured under dry conditions at 30 °C and higher. As the drift gas water concentration increased, $[IsoF•CO_3]^-$ became more unstable and survived until approximately 150 ppmv H_2O between 25 and 40 °C. $[IsoF•CO_3]^-$ was not observed above approximately 75 ppmv H_2O at 50 °C.

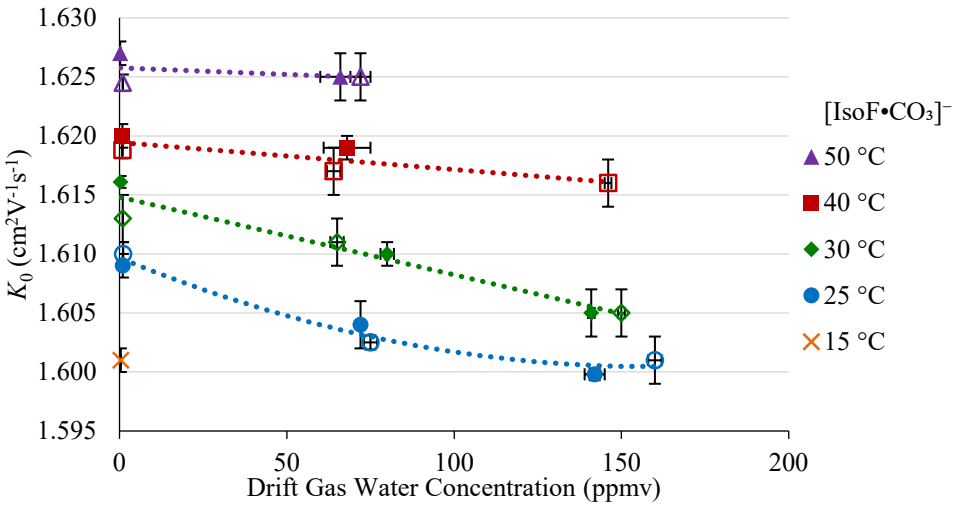

Figure 5. Effect of drift gas water concentration on the K_0 value for $[IsoF•CO_3]^-$ in IMMS mode at five drift gas temperatures under ammonia-doped (solid marker) and undoped (open marker) conditions.

3.2.3 $[(IsoF)_2 \bullet O_2]^-$ Dimer

Figure 6 shows the effects of drift gas temperature and water concentration on the K_0 value for the $[(IsoF)_2 \bullet O_2]^-$ dimer under both ammonia-doped (solid marker) and undoped (open marker) conditions. The previously described effects of drift gas water concentration on the formation of the dimer ion and the resulting low signal limited the range of operational conditions at which the K_0 value could be measured in both instrumentation modes. The black dashed trend line in the plot is the overall trend line for all data points. The trend line has a positive slope because the previously described metastable ion complexes created an asymmetrical drift time peak on its leading edge. This asymmetry shifted the peak centroid and was only evident upon close examination of the spectra and in the calculation of the K_0 values. However, the effect could be mitigated in IMMS mode by increasing the centroid threshold. K_0 values for $[(IsoF)_2 \bullet O_2]^-$ measured in standalone IMS mode under the same drift gas conditions (shown in appendix Figure A-3) featured a more prominent positive slope when plotted, due to the lower resolving power. Still, the K_0 values measured in standalone IMS mode were consistent with the values and trends reported in Figure 6.

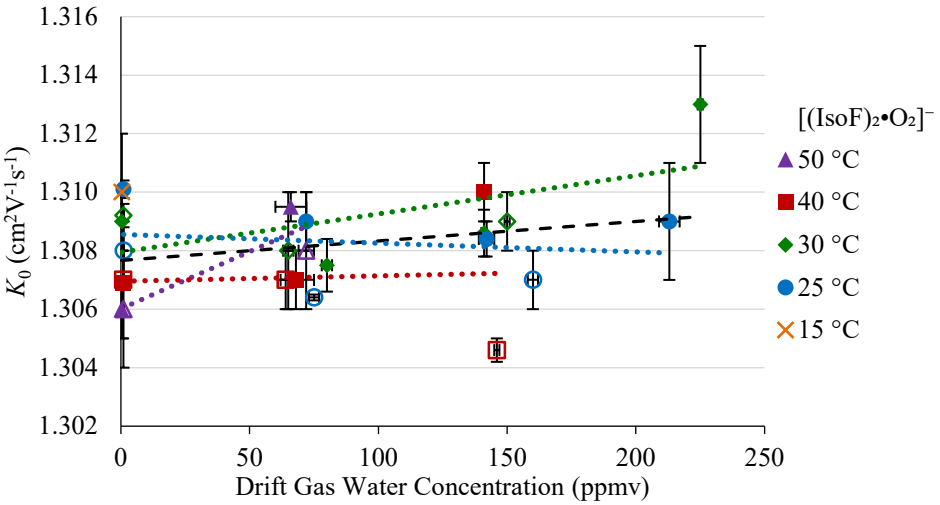

Figure 6. Effect of drift gas water concentration on the K_0 value for $[(IsoF)_2 \bullet O_2]^-$ dimer in IMMS mode at five drift gas temperatures under ammonia-doped (solid marker) and undoped (open marker) conditions.

Regardless of the effect of drift gas water concentration on the formation of $[(IsoF)_2 \bullet O_2]^-$, the K_0 value for the ion was consistent within and across each instrumentation mode. The average K_0 values for $[(IsoF)_2 \bullet O_2]^-$ as measured in the IMMS and standalone IMS modes were 1.308 ± 0.002 and 1.308 ± 0.001 $cm^2V^{-1}s^{-1}$, respectively. The overall average of all K_0 value measurements for $[(IsoF)_2 \bullet O_2]^-$ was 1.308 ± 0.002 $cm^2V^{-1}s^{-1}$. Eiceman and colleagues[6] and González-Méndez and colleagues[7] reported K_0 values of 1.30 and 1.22 $cm^2V^{-1}s^{-1}$, respectively, for $[(IsoF)_2 \bullet O_2]^-$. The difference between our reported values and the values reported by Eiceman and colleagues and González-Méndez and colleagues were 0.6 and 7.0%, respectively. The K_0 value for $[(IsoF)_2 \bullet O_2]^-$ as reported by Eiceman and colleagues was from a

chloride-doped system. However, due to the sterically protected charge site on the $[(IsoF)_2 \bullet O_2]^-$ dimer, the chloride dopant did not affect the product ion chemistry or K_0 value. Therefore, there is good agreement between their reported K_0 value and ours for $[(IsoF)_2 \bullet O_2]^-$. There is no clear reason for the large difference between our reported value and the K_0 value for $[(IsoF)_2 \bullet O_2]^-$ as reported by González-Méndez and colleagues. However, it is possible that measurement and gradient inaccuracies existed in the drift gas temperature of the instrument used by González-Méndez and colleagues because they stated that the drift gas was controlled, but not measured, to within 30 ± 1 °C.

3.2.4 Effect of Increasing Drift Gas Temperature under Dry Conditions

We gained additional knowledge from plotting the K_0 values for product ions as a function of increasing temperature of the non-humidified drift gas, as shown in Figure 7. For all data shown in Figure 7, the drift gas water concentration was less than 1.25 ppmv H_2O. As in previous figures, solid markers represent values that were measured under ammonia-doped conditions, and open markers represent values that were measured under undoped conditions. The colored dotted trend lines in each plot correspond with the matching IMMS or standalone IMS instrumentation mode data sets. The black dashed trend lines in each plot take into account all data points for the associated product ion. The K_0 values for both monomer product ions ($[IsoF \bullet O_2]^-$ and $[IsoF \bullet CO_3]^-$) increased as drift gas temperature increased due to higher thermal energy of the ion and a decrease in the small degree of clustering with neutral water molecules that occurred even under these dry conditions. However, the trend lines in Figure 7b have clearly negative slopes. This indicated that the collision cross section of $[(IsoF)_2 \bullet O_2]^-$ increased as drift gas temperature increased, even though all plotted K_0 values were within an overall average of 1.308 ± 0.002 $cm^2V^{-1}s^{-1}$. González-Méndez and colleagues[7] reported that the stable structure of $[IsoF \bullet O_2]^-$ forms through the attachment of the oxygen molecule to the two hydrogens of the IsoF molecule. To create the dimer product ion, the logical continuation of this structure would be for the second IsoF molecule to attach in the same manner on the opposite side of the oxygen molecule. However, one of those hydrogens in IsoF is attached to a stereocenter. Therefore, the IsoF dimer ion can be formed from either a racemic or enantiopure combination of monomers. These various enantiomeric combinations may have varying thermodynamic stabilities, and an increase in drift gas temperature may favor the formation of one dimeric form over others or cause a conformational change in the dimers present. This would account for the observed inverse relationship between drift gas temperature and the K_0 value for $[(IsoF)_2 \bullet O_2]^-$. A thorough investigation of the thermodynamic properties and molecular modeling simulations of $[(IsoF)_2 \bullet O_2]^-$ would further inform these behaviors.

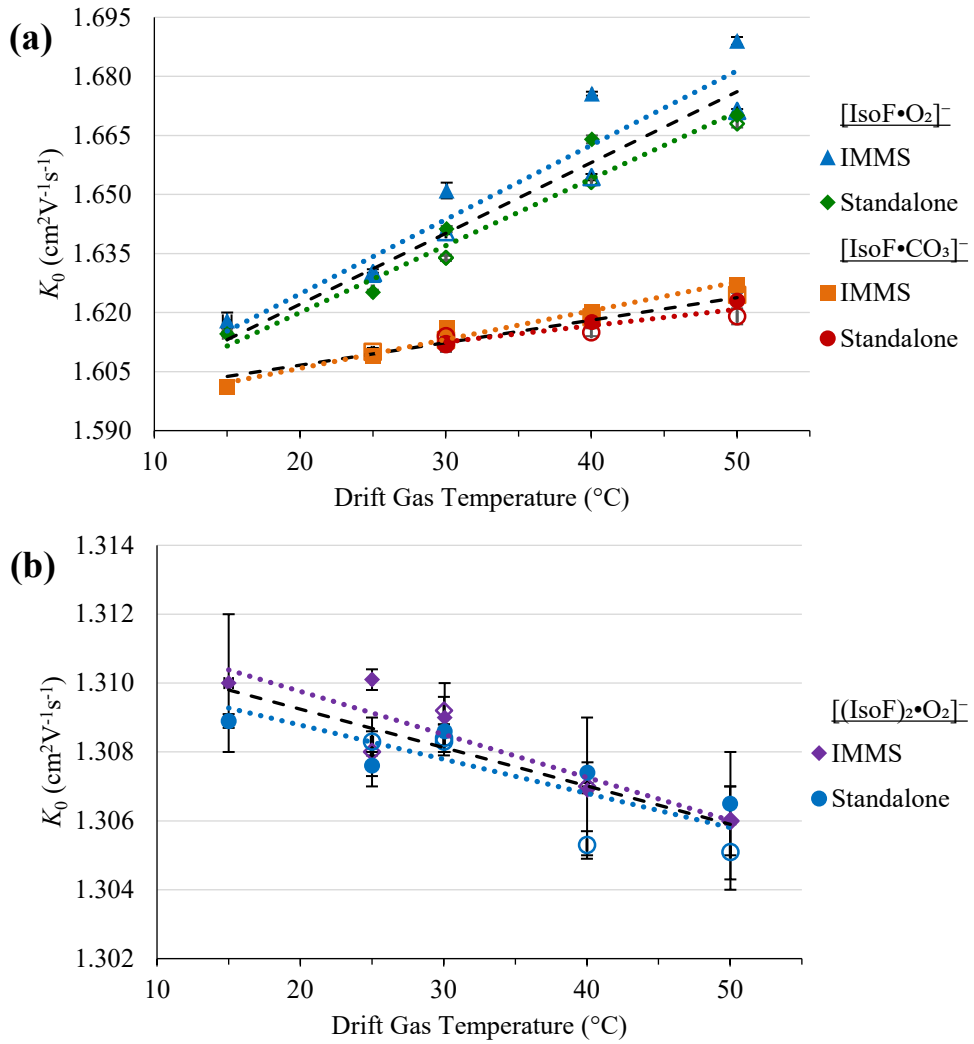

Figure 7. Effect of temperature on the K_0 values for (a) $[IsoF•O_2]^-$ and $[IsoF•CO_3]^-$ and (b) $[(IsoF)_2•O_2]^-$ in IMMS and standalone IMS modes under ammonia-doped (solid marker) and undoped (open marker) conditions with less than 1.25 ppmv H_2O.

4. CONCLUSIONS

The K_0 values for three IsoF product ions were analyzed as a function of drift gas temperature, water concentration, and ammonia dopant concentration to examine the effect of each instrumental parameter. K_0 values were measured in the IMMS and the standalone IMS modes to identify any differences in spectra and measured K_0 values between the two instrumentation modes. The ammonia dopant concentration did not affect the identity of any product ions or their K_0 values. Data from the two instrumentation modes were consistent; between them, only slight differences in measured K_0 values were identified, and these were due to differences in spectral resolving power. The K_0 values for both observed IsoF monomer species, $[IsoF•O_2]^-$ and $[IsoF•CO_3]^-$, were dependent on the temperature and water concentration of the drift gas. Effects of these two instrumental parameters on the K_0 value for the dimer ion, $[(IsoF)_2•O_2]^-$, were minimal. A decrease in spectral resolving power as drift gas water

concentration increased caused the measured K_0 value for $[(IsoF)_2 \bullet O_2]^-$ to increase. The K_0 value for $[(IsoF)_2 \bullet O_2]^-$ also decreased as drift gas temperature increased, and this was most likely due to an increase in collision cross section caused by an enantiomeric or conformational shift in the form of the ion. However, the $[(IsoF)_2 \bullet O_2]^-$ dimer maintained an overall average K_0 value of 1.308 ± 0.002 $cm^2V^{-1}s^{-1}$ for all measurements. An increase in drift gas water concentration created unstable product ion complexes with neutral water molecules and resulted in bridging between drift time peaks. Thus, the K_0 values for $[IsoF \bullet O_2]^-$ and $[(IsoF)_2 \bullet O_2]^-$ can be used to empirically quantify a limited range of drift gas water concentrations during calibration. When all three product ions were stable, an increase in IsoF vapor concentration shifted the ion signal between the two closely spaced monomer drift time peaks. Therefore, IsoF is a suitable calibrant for the negative ion detection mode of IMS under the following conditions. First, a sufficient drying agent should be used for the drift gas to prevent the introduction of ambient water vapor into the drift tube. Second, the calibration algorithm should be programmed to use spectra with monomer-to-dimer peak height ratios that do not correspond to a shift in product ion identity from $[IsoF \bullet O_2]^-$ to $[IsoF \bullet CO_3]^-$ at high IsoF vapor concentrations. Finally, because of these humidity and IsoF vapor concentration effects, the standalone IMS values reported here should be used for calibrating field-deployed IMS-based detectors, given their similar resolving power and inability to separate the two monomer drift time peaks.

LITERATURE CITED

1. Eiceman, G.A.; Stone, J.A. Ion Mobility Spectrometers in National Defense. *Anal. Chem.* **2004,** *76* (21), 390A–397A.

2. Eiceman, G.A.; Karpas, Z.; Hill, H.H., Jr. *Ion Mobility Spectrometry*, 3rd ed.; CRC Press: Boca Raton, FL, 2014.

3. Ewing, R.G.; Atkinson, D.A.; Eiceman, G.A.; Ewing, G.J. A Critical Review of Ion Mobility Spectrometry for the Detection of Explosives and Explosive Related Compounds. *Talanta* **2001,** *54* (3), 515–529.

4. Hauck, B.C.; Harden, C.S.; McHugh, V.M. Current Status and Need for Standards in Ion Mobility Spectrometry. *Int. J. Ion Mobil. Spectrom.* **2018,** *21,* 105–123.

5. Hauck, B.C.; Harden, C.S.; McHugh, V.M. Accurate Evaluation of Potential Calibration Standards for Ion Mobility Spectrometry. *Anal. Chem.* **2020,** *92* (8), 6158–6165.

6. Eiceman, G.A.; Shoff, D.B.; Harden, C.S.; Snyder, A.P.; Fleischer, M.E.; Martinez, P.M.; Watkins, M.L. Ion Mobility Spectrometry of Halothane, Enflurane, and Isoflurane Anesthetics in Air and Respired Gases. *Anal. Chem.* **1989,** *61,* 1093–1099.

7. González-Méndez, R.; Watts, P.; Howse, D.C.; Procino, I.; McIntyre, H.; Mayhew, C.A. Ion Mobility Studies on the Negative Ion-Molecule Chemistry of Isoflurane and Enflurane. *J. Am. Soc. Mass Spectrom.* **2017,** *28,* 939–946.

8. Hauck, B.C.; Siems, W.F.; Harden, C.S.; McHugh, V.M.; Hill, H.H., Jr. Construction and Evaluation of a Hermetically Sealed Accurate Ion Mobility Instrument. *Int. J. Ion Mobil. Spectrom.* **2017,** *20* (3–4), 57–66.

9. Davis, E.J.; Clowers, B.H.; Siems, W.F.; Hill, H.H., Jr. Comprehensive Software Suite for the Operation, Maintenance, and Evaluation of an Ion Mobility Spectrometer. *Int. J. Ion Mobil. Spectrom.* **2011,** *14,* 117–124.

10. González-Méndez, R.; Watts, P.; Howse, D.C.; Procino, I.; McIntyre, H.; Mayhew, C.A. Ion Mobility Studies on the Negative Ion-Molecule Chemistry of Pentachloroethane. *Int. J. Mass Spectrom.* **2017,** *417,* 16–21.

Blank

ACRONYMS AND ABBREVIATIONS

AIMI	Accurate Ion Mobility Instrument
BN	Bradbury–Nielson
DPM	di(propylene glycol) methyl ether
D*t*BP	2,6-di-*tert*-butylpyridine
HPLC	high-performance liquid chromatography
IMMS	ion mobility–mass spectrometry
IMS	ion mobility spectrometry
IMS-	ion mobility spectrometry
IsoF	isoflurane
$[IsoF•CO_3]^-$	carbonate adduct of isoflurane
$[IsoF•NO_2]^-$	nitrate adduct of isoflurane
$[IsoF•O_2]^-$	oxygen adduct of isoflurane
$[(IsoF)_2•O_2]^-$	oxygen-bound dimer of isoflurane
K_0	reduced ion mobility
K_{0cal}	reduced ion mobility of calibrant calculated by an uncalibrated instrument
K_{0det}	calibrated reduced ion mobility of a chemical of interest to be used for identification and alarm detection purposes
K_{0obs}	initially calculated reduced ion mobility of a chemical of interest or unknown peak
K_{0std}	reduced ion mobility of a calibrant standard
L	ion drift length
MES	methyl salicylate
m/z	mass-to-charge ratio
P	drift gas pressure
T	drift gas temperature
t_d	ion drift time
TOFMS	time-of-flight mass spectrometry
V	drift voltage gradient

Blank

APPENDIX:
SUPPLEMENTAL INFORMATION

A.1 SUPPLEMENTAL FIGURES

A schematic of the Accurate Ion Mobility Instrument (AIMI) system and its components is shown in Figure A-1. The figures created from accurate reduced ion mobility (K_0) values measured in standalone ion mobility spectrometry (IMS) mode, corroborating the values measured in ion mobility–mass spectrometry (IMMS) mode in Figures 4 and 6, are shown in Figures A-2 and A-3, respectively.

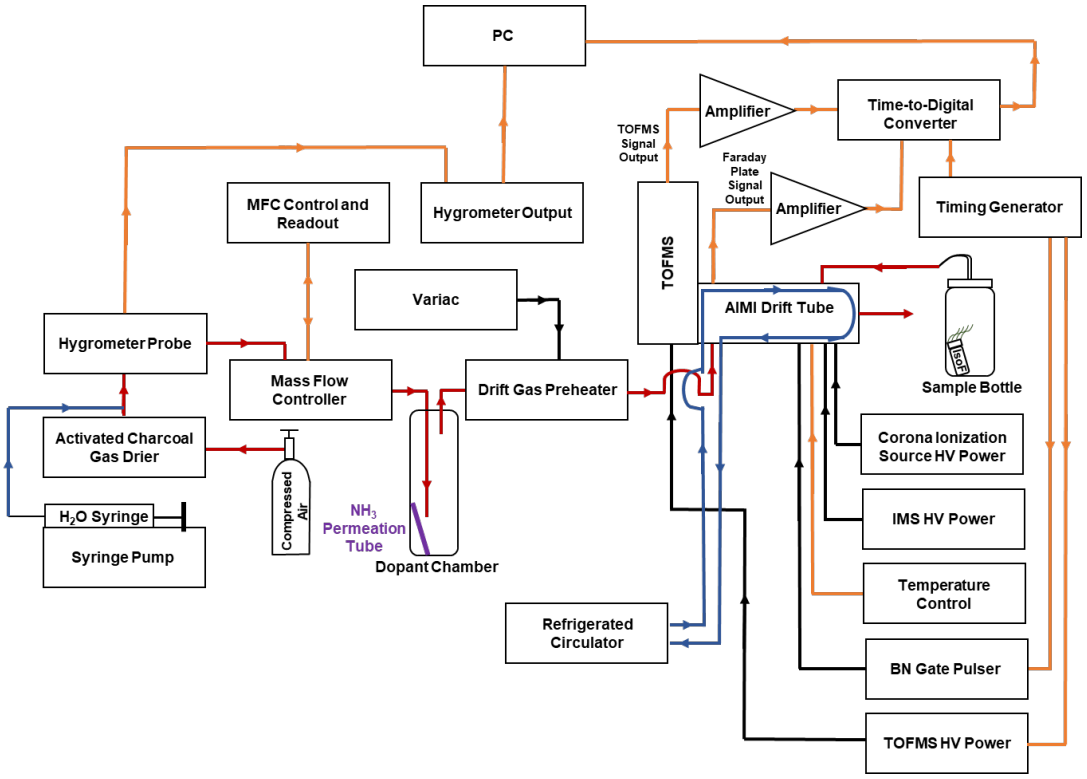

Figure A-1. AIMI system and its components. Red arrows, flows of gas; blue arrows, flows of liquid; orange arrows, electrical control and signal; and black arrows, voltage power. TOFMS, time-of-flight mass spectrometry; HV, high voltage; BN, Bradbury–Nielson.

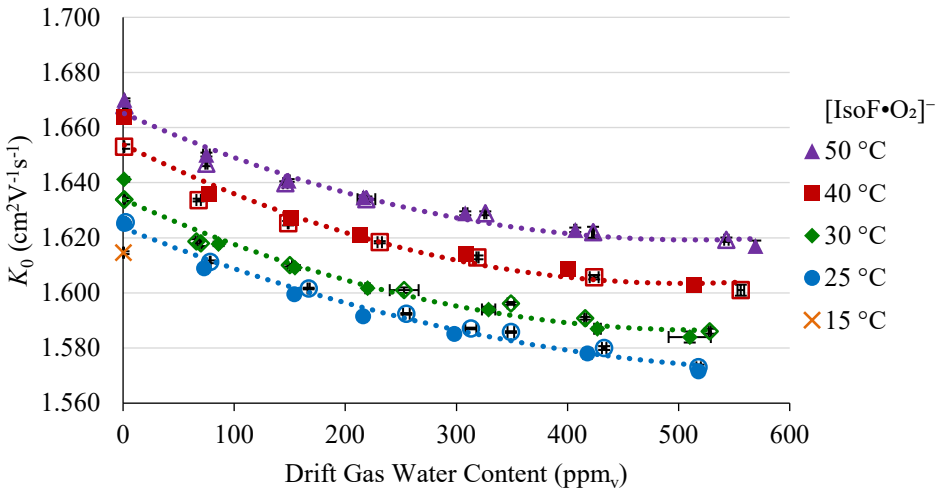

Figure A-2. Effect of drift gas water concentration on the K_0 value for the oxygen adduct of isoflurane, $[IsoF•O_2]^-$, in standalone IMS mode at five drift gas temperatures under ammonia-doped (solid marker) and undoped (open marker) conditions.

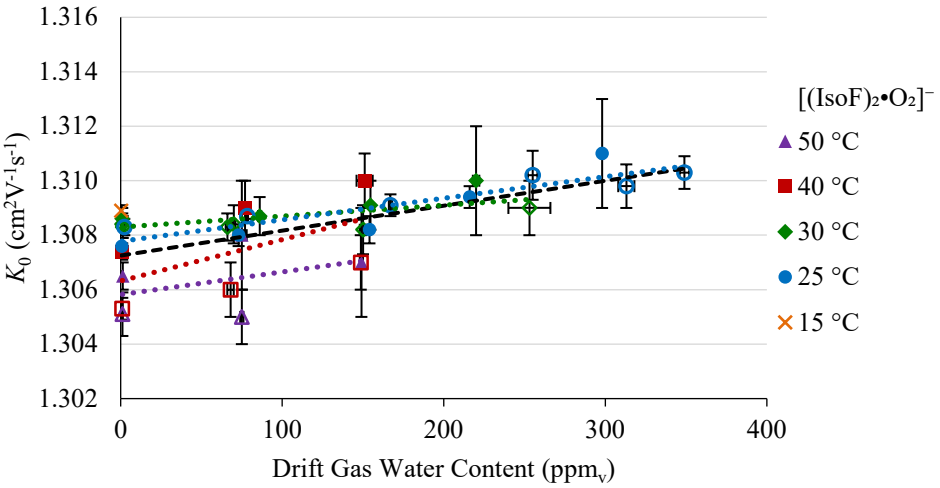

Figure A-3. Effect of drift gas water concentration on the K_0 value for the oxygen-bound dimer of isoflurane, $[(IsoF)_2•O_2]^-$, in standalone IMS mode at five drift gas temperatures under ammonia-doped (solid marker) and undoped (open marker) conditions.

A.2 ACCURATE K_0 VALUES

The accurate K_0 values for the isoflurane (IsoF) product ions (used to create Figures 4–7, A-2, and A-3) are shown in Tables A-1 through A-8. A low-intensity nitrate adduct of isoflurane, $[IsoF{\bullet}NO_2]^-$, product ion peak was observed in IMMS mode when the Bradbury–Nielson ion gates were left open. K_0 values for the $[IsoF{\bullet}NO_2]^-$ product ion are not reported because of the great amount of time that would be required to collect sufficient signal. Each K_0 value is an average of at least three measurements, and precision is represented by error bars in the figures (when not visible, error bars are hidden by the marker).

Table A-1. K_0 Values for $[IsoF{\bullet}O_2]^-$ and $[(IsoF)_2{\bullet}O_2]^-$ on IMS–TOFMS at 280.1 V/cm as a Function of Drift Gas Water Concentration at Four Drift Gas Temperatures under Undoped Conditions

Average Drift Gas Temperature (°C)	**Average Drift Gas Water Concentration (ppmv H_2O)**	**K_0 Value (Precision, Accuracy) ($cm^2V^{-1}s^{-1}$)**	
		$[IsoF{\bullet}O_2]^-$ *m/z* 216, 218	**$[(IsoF)_2{\bullet}O_2]^-$ *m/z* 400, 402**
25.00 ± 0.08	1.07 ± 0.02	1.630 (±0.001, ±0.002)	1.308 (±0.001, ±0.001)
	75 ± 2	1.616 (±0.001, ±0.002)	1.3064 (±0.0001, ±0.001)
	160 ± 2	1.603 (±0.001, ±0.002)	1.307 (±0.001, ±0.001)
	250 ± 7	1.5957 (±0.0006, ±0.002)	N/A
	338 ± 8	1.589 (±0.002, ±0.002)	N/A
	425 ± 10	1.584 (±0.002, ±0.002)	N/A
	510 ± 5	1.581 (±0.002, ±0.002)	N/A
30.02 ± 0.03	1.00 ± 0.02	1.6404 (±0.0005, ±0.002)	1.3092 (±0.0004, ±0.001)
	65 ± 2	1.624 (±0.001, ±0.002)	1.308 (±0.002, ±0.001)
	150 ± 1	1.615 (±0.002, ±0.002)	1.309 (±0.001, ±0.001)
	226 ± 6	1.6063 (±0.0008, ±0.002)	N/A
	358 ± 6	1.5955 (±0.0008, ±0.002)	N/A
	416 ± 5	1.5923 (±0.0006, ±0.002)	N/A
	526 ± 4	1.5880 (±0.0005, ±0.002)	N/A
40.01 ± 0.04	0.84 ± 0.01	1.6544 (±0.0008, ±0.002)	1.307 (±0.002, ±0.001)
	64 ± 2	1.6370 (±0.0003, ±0.002)	1.307 (±0.001, ±0.001)
	146 ± 1	1.6281 (±0.0008, ±0.002)	1.3046 (±0.0004, ±0.001)
	227 ± 8	1.6225 (±0.0006, ±0.002)	N/A
	296 ± 1	1.617 (±0.001, ±0.002)	N/A
	419 ± 3	1.611 (±0.002, ±0.002)	N/A
	513 ± 5	1.606 (±0.001, ±0.002)	N/A
50.01 ± 0.04	1.00 ± 0.01	1.6712 (±0.0005, ±0.002)	1.306 (±0.002, ±0.001)
	72 ± 3	1.651 (±0.001, ±0.002)	1.308 (±0.002, ±0.001)
	149 ± 1	1.6427 (±0.0002, ±0.002)	N/A
	219.7 ± 0.2	1.636 (±0.002, ±0.002)	N/A
	313 ± 2	1.631 (±0.002, ±0.002)	N/A
	422 ± 3	1.626 (±0.002, ±0.002)	N/A
	546 ± 2	1.621 (±0.002, ±0.002)	N/A

N/A, not applicable.

Table A-2. K_0 Values for $[IsoF•O_2]^-$ and $[(IsoF)_2•O_2]^-$ on IMS–TOFMS at 280.1 V/cm as a Function of Drift Gas Water Concentration at Five Drift Gas Temperatures under Ammonia-Doped Conditions

Average Drift Gas Temperature (°C)	**Average Drift Gas Water Concentration (ppmv H_2O)**	**K_0 Value (Precision, Accuracy) ($cm^2V^{-1}s^{-1}$)**	
		$[IsoF•O_2]^-$ *m/z* 216, 218	**$[(IsoF)_2•O_2]^-$ *m/z* 400, 402**
15.0 ± 0.3	0.389 ± 0.006	1.618 (±0.002, ±0.002)	1.310 (±0.002, ±0.001)
25.00 ± 0.08	1.01 ± 0.02	1.6295 (±0.0006, ±0.002)	1.3101 (±0.0003, ±0.001)
	72 ± 1	1.615 (±0.001, ±0.002)	1.309 (±0.001, ±0.001)
	142 ± 3	1.6044 (±0.0003, ±0.002)	1.3084 (±0.0006, ±0.001)
	213 ± 4	1.5971 (±0.0007, ±0.002)	1.309 (±0.002, ±0.001)
	307 ± 3	1.5898 (±0.0005, ±0.002)	N/A
	399 ± 3	1.582 (±0.002, ±0.002)	N/A
	503 ± 4	1.573 (±0.002, ±0.002)	N/A
30.07 ± 0.03	0.314 ± 0.003	1.651 (±0.002, ±0.002)	1.309 (±0.001, ±0.001)
	80 ± 2	1.6257 (±0.0006, ±0.002)	1.3075 (±0.0009, ±0.001)
	141 ± 1	1.6135 (±0.0008, ±0.002)	1.3086 (±0.0008, ±0.001)
	225 ± 1	1.6060 (±0.0009, ±0.002)	1.313 (±0.002, ±0.001)
	323 ± 2	1.5980 (±0.0004, ±0.002)	N/A
	437 ± 17	1.5906 (±0.0001, ±0.002)	N/A
	518 ± 6	1.5853 (±0.0009, ±0.002)	N/A
40.04 ± 0.02	0.83 ± 0.01	1.6756 (±0.0005, ±0.002)	1.3069 (±0.0001, ±0.001)
	68 ± 7	1.6415 (±0.0007, ±0.002)	1.307 (±0.001, ±0.001)
	141 ± 1	1.632 (±0.001, ±0.002)	1.310 (±0.001, ±0.001)
	216 ± 1	1.625 (±0.001, ±0.002)	N/A
	296 ± 2	1.619 (±0.002, ±0.002)	N/A
	417 ± 1	1.6104 (±0.0006, ±0.002)	N/A
	512 ± 16	1.6073 (±0.0006, ±0.002)	N/A
50.00 ± 0.03	0.25 ± 0.01	1.689 (±0.001, ±0.002)	1.306 (±0.001, ±0.001)
	66 ± 6	1.657 (±0.001, ±0.002)	1.3095 (±0.0005, ±0.001)
	143 ± 1	1.6466 (±0.0007, ±0.002)	N/A
	215 ± 1	1.638 (±0.001, ±0.002)	N/A
	303 ± 2	1.635 (±0.002, ±0.002)	N/A
	425 ± 8	1.6282 (±0.0005, ±0.002)	N/A
	506 ± 9	1.624 (±0.001, ±0.002)	N/A

N/A, not applicable.

Table A-3. K_0 Values for $[IsoF{\bullet}CO_3]^-$ (*m/z* 244, 246) on IMS–TOFMS at 280.1 V/cm as a Function of Drift Gas Water Concentration at Four Drift Gas Temperatures under Undoped Conditions

Average Drift Gas Temperature (°C)	**Average Drift Gas Water Concentration (ppmv H_2O)**	**K_0 Value (Precision, Accuracy) ($cm^2V^{-1}s^{-1}$)**
25.00 ± 0.08	1.07 ± 0.02	1.610 (±0.001, ±0.002)
	75 ± 2	1.6025 (±0.0006, ±0.002)
	160 ± 2	1.601 (±0.002, ±0.002)
30.02 ± 0.03	1.00 ± 0.02	1.613 (±0.002, ±0.002)
	65 ± 2	1.611 (±0.002, ±0.002)
	150 ± 1	1.605 (±0.002, ±0.002)
40.01 ± 0.04	0.84 ± 0.01	1.6188 (±0.0007, ±0.002)
	64 ± 2	1.617 (±0.002, ±0.002)
	146 ± 1	1.616 (±0.002, ±0.002)
50.01 ± 0.04	1.00 ± 0.01	1.6245 (±0.0007, ±0.002)
	72 ± 3	1.625 (±0.002, ±0.002)

Table A-4. K_0 Values for $[IsoF{\bullet}CO_3]^-$ (*m/z* 244, 246) on IMS–TOFMS at 280.1 V/cm as a Function of Drift Gas Water Concentration at Five Drift Gas Temperatures under Ammonia-Doped Conditions

Average Drift Gas Temperature (°C)	**Average Drift Gas Water Concentration (ppmv H_2O)**	**K_0 Value (Precision, Accuracy) ($cm^2V^{-1}s^{-1}$)**
15.0 ± 0.3	0.389 ± 0.006	1.601 (±0.001, ±0.002)
25.00 ± 0.08	1.01 ± 0.02	1.609 (±0.001, ±0.002)
	72 ± 1	1.604 (±0.002, ±0.002)
	142 ± 3	1.5998 (±0.0005, ±0.002)
30.07 ± 0.03	0.314 ± 0.003	1.6161 (±0.0005, ±0.002)
	80 ± 2	1.610 (±0.001, ±0.002)
	141 ± 1	1.605 (±0.002, ±0.002)
40.04 ± 0.02	0.83 ± 0.01	1.620 (±0.001, ±0.002)
	68 ± 7	1.619 (±0.001, ±0.002)
50.00 ± 0.03	0.25 ± 0.01	1.627 (±0.001, ±0.002)
	66 ± 6	1.625 (±0.002, ±0.002)

Table A-5. K_0 Values for First Monomer and Dimer Peaks, Corresponding to $[IsoF•O_2]^-$ and $[(IsoF)_2•O_2]^-$, Respectively, on IMS Faraday Plate at 280.1 V/cm as a Function of Drift Gas Water Concentration at Four Drift Gas Temperatures under Undoped Conditions

Average Drift Gas Temperature (°C)	**Average Drift Gas Water Concentration (ppmv H_2O)**	**K_0 Value (Precision, Accuracy) ($cm^2V^{-1}s^{-1}$)**	
		Monomer Peak 1 $[IsoF•O_2]^-$	**Dimer Peak $[(IsoF)_2•O_2]^-$**
25.00 ± 0.08	2.248 ± 0.004	1.6256 (±0.0002, ±0.002)	1.3083 (±0.0003, ±0.001)
	78.4 ± 0.4	1.6113 (±0.0005, ±0.002)	1.3087 (±0.0001, ±0.001)
	167 ± 1	1.6016 (±0.0003, ±0.002)	1.3091 (±0.0004, ±0.001)
	255 ± 3	1.5924 (±0.0003, ±0.002)	1.3102 (±0.0009, ±0.001)
	313 ± 5	1.5871 (±0.0003, ±0.002)	1.3098 (±0.0008, ±0.001)
	349 ± 3	1.5858 (±0.0003, ±0.002)	1.3103 (±0.0006, ±0.001)
	433 ± 2	1.5800 (±0.0007, ±0.002)	N/A
	518 ± 2	1.573 (±0.001, ±0.002)	N/A
30.02 ± 0.03	0.99 ± 0.02	1.6339 (±0.0008, ±0.002)	1.3084 (±0.0004, ±0.001)
	1.32 ± 0.01	1.6339 (±0.0005, ±0.002)	1.3083 (±0.0004, ±0.001)
	66 ± 1	1.6187 (±0.0008, ±0.002)	1.3083 (±0.0005, ±0.001)
	70 ± 1	1.618 (±0.001, ±0.002)	1.3084 (±0.0007, ±0.001)
	150 ± 2	1.6101 (±0.0005, ±0.002)	1.3082 (±0.0009, ±0.001)
	253 ± 13	1.601 (±0.001, ±0.002)	1.309 (±0.001, ±0.001)
	349 ± 3	1.5962 (±0.0005, ±0.002)	N/A
	416 ± 1	1.5908 (±0.0005, ±0.002)	N/A
	528 ± 1	1.5861 (±0.0009, ±0.002)	N/A
40.00 ± 0.03	1.00 ± 0.01	1.6531 (±0.0008, ±0.002)	1.3053 (±0.0004, ±0.001)
	68 ± 2	1.6337 (±0.0005, ±0.002)	1.306 (±0.001, ±0.001)
	148.6 ± 0.4	1.6253 (±0.0008, ±0.002)	1.307 (±0.001, ±0.001)
	231 ± 2	1.6184 (±0.0004, ±0.002)	N/A
	319 ± 1	1.6129 (±0.0007, ±0.002)	N/A
	424 ± 4	1.6057 (±0.0008, ±0.002)	N/A
	556 ± 3	1.601 (±0.002, ±0.002)	N/A
50.01 ± 0.04	1.06 ± 0.02	1.668 (±0.001, ±0.002)	1.3051 (±0.0008, ±0.001)
	75 ± 1	1.6469 (±0.0009, ±0.002)	1.305 (±0.001, ±0.001)
	146 ± 2	1.6398 (±0.0007, ±0.002)	N/A
	219 ± 8	1.634 (±0.001, ±0.002)	N/A
	326 ± 1	1.6289 (±0.0007, ±0.002)	N/A
	423 ± 1	1.622 (±0.002, ±0.002)	N/A
	543 ± 2	1.6193 (±0.0008, ±0.002)	N/A

N/A, not applicable.

Table A-6. K_0 Values for First Monomer and Dimer Peaks, Corresponding to $[IsoF•O_2]^-$ and $[(IsoF)_2•O_2]^-$, Respectively, on IMS Faraday Plate at 280.2 V/cm as a Function of Drift Gas Water Concentration at Five Drift Gas Temperatures under Ammonia-Doped Conditions

Average Drift Gas Temperature (°C)	**Average Drift Gas Water Concentration (ppmv H_2O)**	**K_0 Value (Precision, Accuracy) ($cm^2V^{-1}s^{-1}$)**	
		Monomer Peak 1 $[IsoF•O_2]^-$	**Dimer Peak $[(IsoF)_2•O_2]^-$**
15.0 ± 0.3	0.394 ± 0.007	1.6146 (±0.0005, ±0.002)	1.3089 (±0.0002, ±0.001)
25.00 ± 0.08	0.799 ± 0.001	1.6251 (±0.0001, ±0.002)	1.3076 (±0.0003, ±0.001)
	73 ± 3	1.6089 (±0.0005, ±0.002)	1.3080 (±0.0004, ±0.001)
	154 ± 1	1.5995 (±0.0001, ±0.002)	1.3082 (±0.0005, ±0.001)
	216 ± 1	1.5915 (±0.0006, ±0.002)	1.3094 (±0.0004, ±0.001)
	298 ± 1	1.5851 (±0.0006, ±0.002)	1.311 (±0.002, ±0.001)
	418 ± 4	1.578 (±0.001, ±0.002)	N/A
	518 ± 1	1.5715 (±0.0006, ±0.002)	N/A
30.07 ± 0.03	0.99 ± 0.08	1.6412 (±0.0008, ±0.002)	1.3086 (±0.0004, ±0.001)
	86 ± 1	1.6178 (±0.0008, ±0.002)	1.3087 (±0.0007, ±0.001)
	154.6 ± 0.3	1.6092 (±0.0009, ±0.002)	1.3091 (±0.0009, ±0.001)
	220 ± 2	1.6017 (±0.0004, ±0.002)	1.310 (±0.002, ±0.001)
	329 ± 6	1.594 (±0.001, ±0.002)	N/A
	427 ± 3	1.5870 (±0.0005, ±0.002)	N/A
	510 ± 19	1.584 (±0.002, ±0.002)	N/A
40.04 ± 0.02	0.955 ± 0.004	1.664 (±0.001, ±0.002)	1.3074 (±0.0003, ±0.001)
	77 ± 2	1.6358 (±0.0006, ±0.002)	1.309 (±0.001, ±0.001)
	151 ± 5	1.627 (±0.001, ±0.002)	1.310 (±0.001, ±0.001)
	213 ± 1	1.6211 (±0.0006, ±0.002)	N/A
	309.2 ± 0.3	1.614 (±0.001, ±0.002)	N/A
	400 ± 4	1.6086 (±0.0004, ±0.002)	N/A
	514 ± 2	1.603 (±0.001, ±0.002)	N/A
50.00 ± 0.03	1.23 ± 0.01	1.6701 (±0.0005, ±0.002)	1.3065 (±0.0005, ±0.001)
	75 ± 3	1.6502 (±0.0007, ±0.002)	1.308 (±0.002, ±0.001)
	149 ± 1	1.6408 (±0.0005, ±0.002)	1.307 (±0.002, ±0.001)
	216.2 ± 0.3	1.6347 (±0.0007, ±0.002)	N/A
	308 ± 2	1.6289 (±0.0007, ±0.002)	N/A
	407 ± 1	1.6229 (±0.0008, ±0.002)	N/A
	569 ± 1	1.617 (±0.002, ±0.002)	N/A

N/A, not applicable.

Table A-7. K_0 Values for Second Monomer Peak, Corresponding to $[IsoF \bullet CO_3]^-$, on IMS Faraday Plate at 280.1 V/cm as a Function of Drift Gas Water Concentration at Three Drift Gas Temperatures under Undoped Conditions

Average Drift Gas Temperature (°C)	**Average Drift Gas Water Concentration (ppmv H_2O)**	**K_0 Value (Precision, Accuracy) ($cm^2V^{-1}s^{-1}$)**
30.02 ± 0.03	0.99 ± 0.02	1.612 (±0.002, ±0.002)
	1.32 ± 0.01	1.614 (±0.002, ±0.002)
40.00 ± 0.03	1.00 ± 0.01	1.615 (±0.001, ±0.002)
50.01 ± 0.04	1.06 ± 0.02	1.619 (±0.002, ±0.002)

Table A-8. K_0 Values for Second Monomer Peak, Corresponding to $[IsoF \bullet CO_3]^-$, on IMS Faraday Plate at 280.2 V/cm as a Function of Drift Gas Water Concentration at Three Drift Gas Temperatures under Ammonia-Doped Conditions

Average Drift Gas Temperature (°C)	**Average Drift Gas Water Concentration (ppmv H_2O)**	**K_0 Value (Precision, Accuracy) ($cm^2V^{-1}s^{-1}$)**
30.07 ± 0.03	0.99 ± 0.08	1.612 (±0.001, ±0.002)
40.04 ± 0.02	0.955 ± 0.004	1.6176 (±0.0009, ±0.002)
50.00 ± 0.03	1.23 ± 0.01	1.623 (±0.002, ±0.002)

DISTRIBUTION LIST

The following individuals and organizations were provided with one Adobe portable document format (pdf) electronic version of this report:

U.S. Combat Capabilities Development Command Chemical Biological Center (DEVCOM CBC)
FCDD-CBR-ID
ATTN: Hauck, B.
McHugh, V.
Harden, C.
Wade, M.

DEVCOM CBC Technical Library
FCDD-CBR-L
ATTN: Foppiano, S.
Stein, J.

Defense Technical Information Center
ATTN: DTIC OA

Joint Project Manager for Chemical, Biological, Radiological and Nuclear Sensors (JPM CBRN Sensors)
ATTN: Matz, C.
Powers, M.
Gauani, H.

U.S. ARMY COMBAT CAPABILITIES DEVELOPMENT COMMAND
CHEMICAL BIOLOGICAL CENTER